


Prognostic value of post-procedural μ QFR for drug-coated balloons in the treatment of in-stent restenosis

Lili Liu¹ , Fenghua Ding¹, Juan Luis Gutiérrez-Chico¹,
 Jinzhou Zhu¹, Zhengbin Zhu¹, Run Du¹, Zhenkun Yang¹, Jian Hu¹,
 Shengxian Tu², Ruiyan Zhang¹

¹Department of Cardiovascular Medicine, Ruijin Hospital,
 Shanghai Jiao Tong University School of Medicine, Shanghai, China
²Biomedical Instrument Institute, School of Biomedical Engineering,
 Shanghai Jiao Tong University, Shanghai, China

The paper was guest edited by Prof. Carlos Cortés

Abstract

Background: Investigating the prognostic value of the Murray law-based quantitative flow ratio (μ QFR) on the clinical outcome after treatment of in-stent restenosis (ISR) with a drug-coated balloon (DCB).

Methods: Patients participating in a previous randomized clinical trial for DCB-ISR were post-hoc analyzed. The primary endpoint was vessel-oriented composite endpoint (VOCE), defined as cardiac death, target vessel-related myocardial infarction, and ischemia-driven target vessel revascularization. μ QFRs at baseline and after DCB angioplasty was calculated, and its prognostic value as a predictor of VOCE was explored in Cox regression.

Results: A total of 169 lesions in 169 patients were analyzed. At 1-year follow-up, 20 VOCEs occurred in 20 patients. Receiver-operating characteristic curve analysis identified a post-procedural μ QFR of ≤ 0.89 as the best cut-off to predict VOCE (area under curve [AUC]: 0.74; 95% confidence interval [CI]: 0.67–0.80; $p < 0.001$), superior to post-procedural in-stent percent diameter stenosis, which reported an AUC of 0.61 (95% CI: 0.53–0.68; $p = 0.18$). Post-procedural μ QFR was significantly lower in patients with VOCE compared with those without (0.88 [interquartile range: 0.79–0.94] vs. 0.96 [interquartile range: 0.91–0.98], respectively; $p < 0.001$). After correction for potential confounders, post-procedural μ QFR ≤ 0.89 was associated with a 6-fold higher risk of VOCE than lesions with μ QFR > 0.89 (hazard ratio: 5.94; 95% CI: 2.33–15.09; $p < 0.001$).

Conclusions: Post-procedural μ QFR may become a promising predictor of clinical outcome after treatment of DES-ISR lesions by DCB angioplasty. (Cardiol J 2023; 30, 2: 167–177)

Key words: quantitative flow ratio, drug-coated balloon, in-stent restenosis

Address for correspondence: Ruiyan Zhang, MD, PhD, FACC, FESC, Department of Cardiovascular Medicine, Ruijin Hospital, Shanghai Jiao Tong University School of Medicine, No. 197, Ruijin Second Road, Shanghai, 200025, China, tel: +86 21 64370045, fax: +86 21 64457177, e-mail: zhangruiyan@263.net; Shengxian Tu, PhD, FACC, FESC, Med-X Research Institute, Shanghai Jiao Tong University, No. 1954, Huashan Road, Shanghai, 200030, China, tel: +86 21 62932631, e-mail: sxtu@sjtu.edu.cn

Received: 10.09.2021

Accepted: 9.11.2021

Early publication date: 19.11.2021

This article is available in open access under Creative Commons Attribution-Non-Commercial-No Derivatives 4.0 International (CC BY-NC-ND 4.0) license, allowing to download articles and share them with others as long as they credit the authors and the publisher, but without permission to change them in any way or use them commercially.

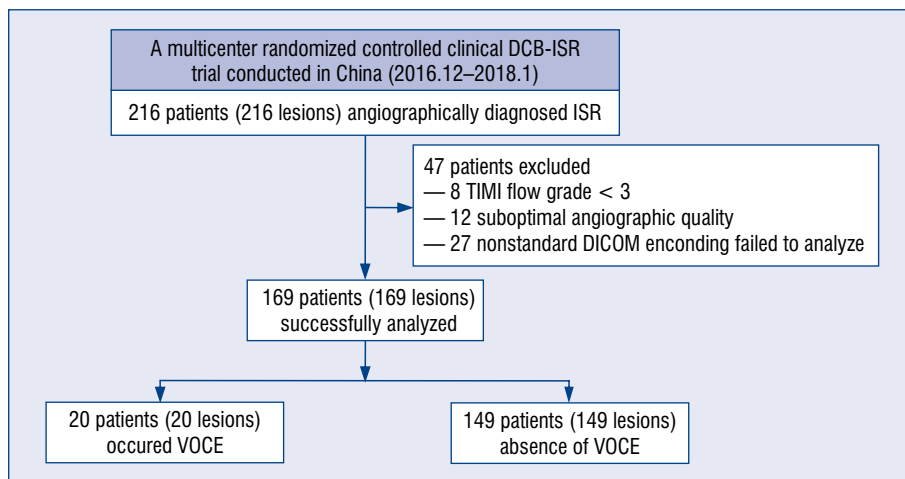


Figure 1. Flow chart of this study; DCB — drug-coated balloon; ISR — in-stent restenosis; μ QFR — Murray law-based quantitative flow ratio; TIMI — thrombolysis in myocardial infarction; VOCE — vessel-oriented composite endpoint.

Introduction

Second-generation drug eluting stents (DES) have effectively inhibited neointimal hyperplasia and hence substantially reduced the incidence of in-stent restenosis (ISR) [1, 2]. Nonetheless, recurrent ISR still occurs in late or very late phases after DES implantation in up to 7–10% of cases [3, 4], and interventional treatment of DES-ISR remains challenging. Several studies have demonstrated the efficacy of drug-coated balloons (DCB) for the treatment of ISR [5–9]. DCBs transfer an antiproliferative drug, in most cases paclitaxel, onto the vessel wall during the short time of balloon inflation, resulting in efficient inhibition of smooth muscle cell proliferation and neointimal hyperplasia [10, 11], thus circumventing the need to implant additional metallic layers in the vessel, whilst achieving a comparable net therapeutic performance to DES [9, 12, 13].

Quantitative flow ratio (QFR) is an innovative implement of computational physiology based on three-dimensional (3D) reconstruction of anatomy and hemodynamic simulation, which has shown excellent correlation and agreement with invasive wire-based fractional flow reserve (FFR) [14–16]. Previous studies have demonstrated that QFR can be used to evaluate patients with ISR [17, 18], and post-procedural QFR had the ability to predict future clinical vessel-oriented composite endpoints (VOCE) [19]. On this basis, several studies have recently explored the ability of conventional 3D-based QFR to predict the clinical outcome of ISR

treated with DCB [20, 21]. Our current study appraised the prognostic value of the new-generation QFR, based on Murray bifurcation fractal law (μ QFR), aided by artificial intelligence [22], to predict the incidence of vessel-oriented composite endpoint after DCB angioplasty, using data from a previous DCB-ISR trial.

Methods

Study design

This was a post-hoc analysis of a prospective, multicenter, randomized controlled clinical trial comparing the efficacy of two different kinds of DCBs, Shenqi (Shenqi Medical, Shanghai, China) or Sequent Please (B. Braun Melsungen AG, Melsungen, Germany), for the treatment of first-occurrence DES-ISR between December 2016 and January 2018 [11]. Patients were excluded from the current analysis if the thrombolysis in myocardial infarction (TIMI) grade flow was < 3 at baseline or after DCB angioplasty, the angiography recordings were deemed of insufficient quality for μ QFR analysis, or nonstandard angiographic DICOM imaging encoding failed to analyze μ QFR (Fig. 1).

The study complied with the principles of good clinical practice and with the Declaration of Helsinki for investigation in human beings. The study protocol was approved by the Institutional Review Board and Ethics Committee at each participating center, and all patients provided written informed consent before receiving DCB treatment.

Angiographic follow-up and endpoint definition

Patients were routinely scheduled an angiographic follow-up of 9 ± 1 months, even though some angiograms were performed earlier or later if clinically indicated. The endpoint of the study was VOCE at 1-year follow-up, defined as a composite of cardiac death, target vessel-related myocardial infarction, and ischemia-driven target vessel revascularization (TVR). A residual lesion was defined as diameter stenosis (DS) $\geq 50\%$ in vessels ≥ 1.5 mm by visual assessment, not located within the in-segment (a ISR lesion complete treated segment + 5 mm adjacent margins) treatment by DCB angioplasty.

Quantitative coronary angiography (QCA)

Quantitative measurements of coronary angiograms were analyzed offline using QAngio XA 7.3 (Medis Medical Imaging System BV, Leiden, the Netherlands) by two well-trained observers, blind to patients' information, at the central angiographic core laboratory, according to standard methodology [11]. Appropriate angiographic projections were selected to avoid excessive vessel foreshortening and overlap. Reference and minimal lumen diameters, percentage of DS, and lesion length were measured before and immediately after the procedure, and at follow-up. Restenosis patterns were assessed by Mehran classification [23].

μ QFR computation

Two experienced and qualified analysts performed μ QFR analysis offline, using Angioplus Galley software (Pulse Medical Imaging Technology, Shanghai, China). A single angiographic projection displaying the target vessel from the ostium to the distal segment, with the corresponding side branches and encompassing the whole target lesion, was selected as meeting the requirements of μ QFR analysis. The frame with optimal definition of the target lesion was chosen as the key frame for the measurements. Lumen contour and coronary flow velocity were automatically delineated and computed, respectively, aided by artificial intelligence. In cases of inaccurate lumen delineation, minor manual editing was allowed by adding additional points markers along the lumen contour. The reference diameter was calculated along the target vessel according to the Murray fractal law, resulting in reference step-down at bifurcations. Then the physiological indexes of the main vessel and side branch were subsequently derived. In the presence of an eccentric lesion, 3D QCA analysis was performed after selecting a second

projection of the target vessel, $> 25^\circ$ apart from the main projection. 3D μ QFR was computed from the reconstruction used for 3D-QCA. A paradigmatic example is shown in Figure 2.

Statistical analysis

Continuous variables were expressed as mean \pm standard deviation or median (interquartile range) according to the data distribution determined by the Kolmogorov-Smirnov test, and they were compared using Student's t-test or the Mann-Whitney U test, as appropriate. Categorical variables were described as counts (percentage) and compared using Pearson's χ^2 test or Fisher's exact test, as appropriate. Receiver operator characteristic (ROC) curve analysis was performed to determine the optimal post-procedural μ QFR cut-off value to predict VOCE, as determined by the Youden index. Kaplan-Meier survival analysis was performed, comparing the groups defined by the μ QFR cut-off with the log-rank test. Multivariate Cox regression analysis was performed to search for independent predictors of VOCE. Proportional-hazards assumption was tested on the basis of Schoenfeld residuals. Hazard ratios (HR) and 95% confidence intervals (CI) were calculated. All statistical analyses were performed using SPSS version 22.0.0 (IBM Corporation, Armonk, New York, USA) and MedCalc version 14.12 (MedCalc Software, Ostend, Belgium). A two-sided p-value < 0.05 was considered as statistically significant.

Results

The study comprised 216 lesions in 216 patients. Forty-seven patients were excluded from the current study due to TIMI grade flow < 3 at baseline or after DCB angioplasty (8 patients), or due to insufficient quality (12 patients) or nonstandard angiographic DICOM imaging encoding (27 patients) for μ QFR analysis, thus resulting in 169 patients being successfully analyzed: 20 patients with VOCE and 149 patients without VOCE (Fig. 1). One-year clinical follow-up was completed in all eligible patients with a median follow-up period of 353 days (340–371 days).

Baseline characteristics

Baseline clinical and procedural characteristics of 169 patients and lesions finally enrolled in the study are presented in Tables 1 and 2. VOCEs occurred in 20 patients at 1-year follow-up. There were no significant differences in age, gender, body mass index, hypertension, hyperlipidemia, current

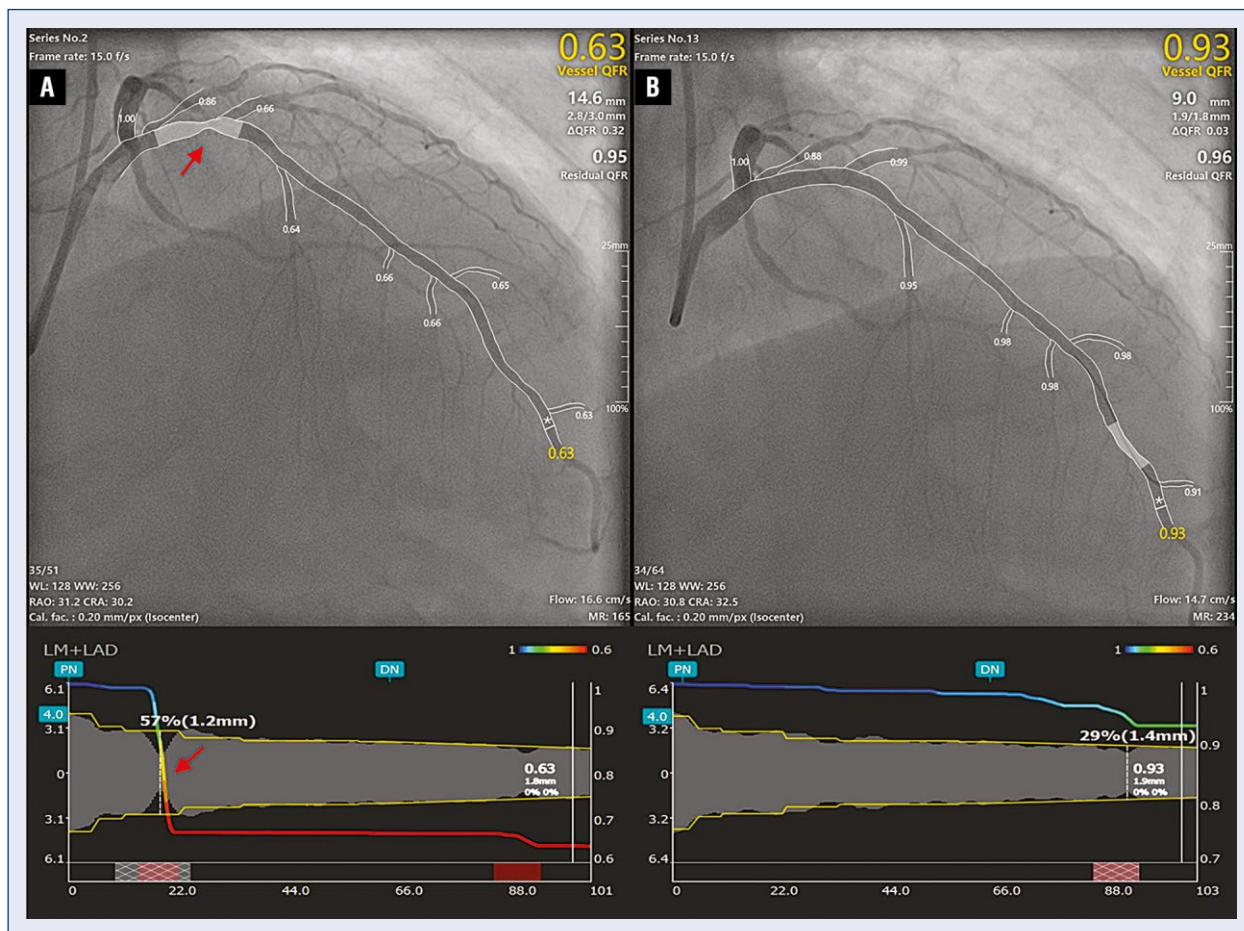


Figure 2. Paradigmatic example of Murray-law based QFR measurement. Murray law-based quantitative flow ratio (μ QFR) computation was solely derived from one angiographic projection view; the lumen contour and its side branches were automatically delineated; a step-down reference diameter was calculated based on the Murray bifurcation fractal law. The μ QFR values at each position for both the main vessel and its side branches were readily available; **A.** Pre-procedural angiographic image shows an in-stent restenosis lesion (red arrow) at the proximal left anterior descending artery; the μ QFR at the asterisk position was 0.63; **B.** After drug-coated balloon angioplasty minimal residual stenosis was detected, the the final μ QFR was 0.93, as indicated by the asterisk.

smoking, medical history, clinical presentation, left ventricular ejection fraction, and number of diseased arteries between patients with and without VOCE. Diabetes mellitus and family history of coronary heart disease were significantly more prevalent among patients with VOCE than among event-free patients (Table 1).

The distributions of target vessel, ostial lesion, bifurcation lesion, Mehran restenosis pattern, and type of DCB applied did not differ between groups. Baseline QCA parameters showed smaller reference vessel diameter (2.37 ± 0.40 vs. 2.60 ± 0.42 , $p = 0.02$) and minimum lumen diameter (0.74 ± 0.35 vs. 0.95 ± 0.39 , $p = 0.02$) in patients with VOCE than in event-free patients, while the mean lesion length and diameter stenosis at baseline and immediately after the procedure were similar

in both groups. Procedural variables were similar between patients with or without VOCE. Patients with VOCE showed lower μ QFR values than event-free patients, both at baseline ($0.50 [0.37-0.75]$ vs. $0.77 [0.63-0.85]$, $p = 0.001$) and post-procedure ($0.88 [0.79-0.94]$ vs. $0.96 [0.91-0.98]$, $p < 0.001$), whilst μ QFR improvement, defined as difference values between post-procedure and baseline, was larger in the VOCE group ($0.30 [0.18-0.41]$ vs. $0.18 [0.10-0.34]$, $p = 0.01$). The proportion of patients with post-procedural μ QFR ≤ 0.80 was larger in the VOCE group than in the event-free group ($6 [30.00\%]$ vs. $6 [4.03\%]$, $p < 0.001$) (Table 2).

Patients with residual lesion after DCB-ISR treatment were more likely to develop VOCE than patients without residual lesion ($8 [40.00\%]$ vs. $21 [14.09\%]$, $p = 0.01$). Moreover, patients with greater

Table 1. Baseline clinical features of patients with available follow-up angiography suitable for Murray law-based quantitative flow ratio (μ QFR) analysis after drug-coated balloon (DCB) treatment of in-stent restenosis (ISR).

Variables	VOCE (n = 20)	Non-VOCE (n = 149)	P
Age [years]	59.90 \pm 11.57	62.88 \pm 9.58	0.20
Female gender	6 (30.00%)	35 (23.49%)	0.58
BMI [kg/m ²]	25.12 \pm 3.15	25.60 \pm 3.31	0.54
CAD risk factors:			
Diabetes mellitus	13 (65.00%)	56 (37.58%)	0.03
Hypertension	15 (75.00%)	109 (73.15%)	0.86
Hyperlipidemia	9 (45.00%)	49 (32.88%)	0.28
Current smoker	6 (30.00%)	33 (22.15%)	0.59
Medical history:			
Previous MI	9 (45.00%)	64 (42.95%)	0.86
Previous PCI	20 (100.00%)	149 (100.00%)	> 0.999
Family history	6 (30.00%)	14 (9.39%)	0.03
Clinical presentation:			0.25
Silent ischemia	0 (0.00%)	15 (10.07%)	
Stable angina	1 (5.00%)	20 (13.42%)	
Unstable angina	19 (95.00%)	114 (76.51%)	
LVEF [%]	61.40 \pm 7.67	60.56 \pm 7.23	0.63
No. of diseased arteries:			0.86
1	6 (30.00%)	55 (36.91%)	
2	10 (50.00%)	68 (45.64%)	
3	4 (20.00%)	26 (17.45%)	

Values are expressed as mean \pm standard deviation or number (%); BMI — body mass index; CAD — coronary artery disease; MI — myocardial infarction; LVEF — left ventricular ejection fraction; PCI — percutaneous coronary intervention; VOCE — vessel-oriented composite endpoint

differences between DCB diameter and reference vessel diameter (RVD) seemed more prone to develop VOCE (0.61 [0.43–0.82] vs. 0.43 [0.29–0.59], $p = 0.004$). The length mismatch between DCB and lesion was similar between groups (Table 2).

Definition of potential post-procedural cut-off value

Receiver-operating characteristic curve analysis identified post-procedural μ QFR ≤ 0.89 as the optimal cut-off value to predict the occurrence of VOCE, with sensitivity 55% and specificity 74% (AUC: 0.74; 95% CI: 0.67–0.80; $p < 0.001$). Nevertheless, there was no significant predictive value of post-procedural percent diameter stenosis (%DS) for VOCE (AUC: 0.61; 95% CI: 0.53–0.68; $p = 0.18$). The ROC curve for μ QFR improvement also showed moderate predictive value for VOCE, with the best cut-off value > 0.20 , and with sensitivity of 75% and specificity of 58% (AUC: 0.67; 95% CI: 0.60–0.74; $p = 0.001$) (Fig. 3).

Clinical outcomes

Clinical outcomes stratified by post-procedural μ QFR are shown in Table 3. Patients who achieved μ QFR > 0.89 after DCB treatment had significantly fewer VOCEs than those with μ QFR ≤ 0.89 (6.77% vs. 30.55%, $p < 0.001$), mainly attributed to a higher incidence rate of TVR (6.77% vs. 27.78%, $p = 0.001$). Two patients presented with more than one event; both developed target vessel myocardial infarction followed by TVR. One patient with post-procedural μ QFR ≤ 0.89 died of cardiac death, while the other, with post-procedural μ QFR > 0.89 , did not. Kaplan-Meier curves also confirmed that post-procedural μ QFR ≤ 0.89 had a remarkably higher incidence rate of VOCE (Fig. 4).

After correcting for potential confounders (diabetes mellitus, family history, ostial lesion, lesion length, residual lesion, differences in diameter DCB-RVD), post-procedural μ QFR ≤ 0.89 remained associated with a 6-fold increase in the risk of VOCE (adjusted HR: 5.94; 95% CI: 2.33–15.09;

Table 2. Baseline lesion and procedural characteristics with available follow-up angiography suitable for Murray law-based quantitative flow ratio (μ QFR) analysis after drug-coated balloon (DCB) treatment of in-stent restenosis (ISR).

Variables	VOCE (n = 20)	Non-VOCE (n = 149)	P
Target vessel:			0.81
RCA	6 (30.00%)	57 (38.26%)	
LAD	11 (55.00%)	70 (46.98%)	
LCX	3 (15.00%)	22 (14.76%)	
Ostial lesion	2 (10.00%)	4 (2.68%)	0.15
Bifurcation lesion	5 (25.00%)	47 (31.54%)	0.55
Restenosis pattern:			0.41
Mehran I	4 (20.00%)	50 (33.56%)	
Mehran II	13 (65.00%)	73 (48.99%)	
Mehran III	3 (15.00%)	26 (17.45%)	
Shenqi DCB	11 (55.00%)	78 (52.35%)	0.82
QCA parameters:			
Lesion length [mm]	15.67 ± 5.61	14.99 ± 8.39	0.73
RVD [mm]	2.37 ± 0.40	2.60 ± 0.42	0.02
MLD [mm]	0.74 ± 0.35	0.95 ± 0.39	0.02
DS [%]	67.95 ± 12.10	63.20 ± 12.53	0.11
DS after DCB [%]	17.58 ± 15.17	21.11 ± 10.10	0.32
Procedural data:			
Predilation	20 (100.00%)	149 (100.00%)	> 0.999
Cutting balloon	5 (25.00%)	38 (25.50%)	0.96
DCB diameter [mm]	2.87 (2.62–3.50)	3.00 (2.75–3.50)	0.48
DCB length [mm]	20.00 (20.00–25.50)	20.00 (17.00–26.00)	0.91
DCB pressure [atm]	9 (8–9)	9 (8–10)	0.60
DCB Inflation time [s]	60 (60–60)	60 (60–60)	> 0.999
No. of DCB used > 1	1 (5.00%)	3 (2.01%)	0.40
μ QFR measurements:			
Baseline μ QFR	0.50 (0.37–0.75)	0.77 (0.63–0.85)	0.001
Post-procedural μ QFR	0.88 (0.79–0.94)	0.96 (0.91–0.98)	< 0.001
Post-procedural μ QFR ≤ 0.80	6 (30.00%)	6 (4.03%)	< 0.001
μ QFR improvement	0.30 (0.18–0.41)	0.18 (0.10–0.34)	0.01
Residual lesion after DCB treatment	8 (40.00%)	21 (14.09%)	0.01
Diameter difference DCB — RVD	0.61 (0.43–0.82)	0.43 (0.29–0.59)	0.004
Length difference DCB — lesion	6.36 (2.62–9.32)	7.26 (2.65–11.88)	0.59

Values are expressed as mean ± standard deviation median (25th–75th percentile) or number (%); DS — diameter stenosis; LAD — left coronary artery; LCX — left circumflex coronary artery; MLD — minimum lumen diameter; QCA — quantitative coronary angiography; RCA — right coronary artery; RVD — reference vessel diameter; VOCE — vessel-oriented composite endpoint

$p < 0.001$; Table 4, Model a1). μ QFR improvement > 0.20 was also associated with suboptimal clinical result at 1-year follow-up (HR: 3.75; 95% CI: 1.31–10.68, $p = 0.01$; Table 4, Model b1). Considered as a continuous variable, post-procedural μ QFR was associated with a lower incidence of VOCE in the multivariate analysis (HR: 0.34; 95% CI: 0.23–0.51; $p < 0.001$), whereas μ QFR improvement (each 0.10

increase) was associated with a higher incidence of VOCE (HR: 1.31; 95% CI: 1.04–1.66; $p = 0.02$; Table 4, Model a2 and Model b2).

Discussion

To the best of our knowledge, this post-hoc study of a previous DCB-ISR trial investigated

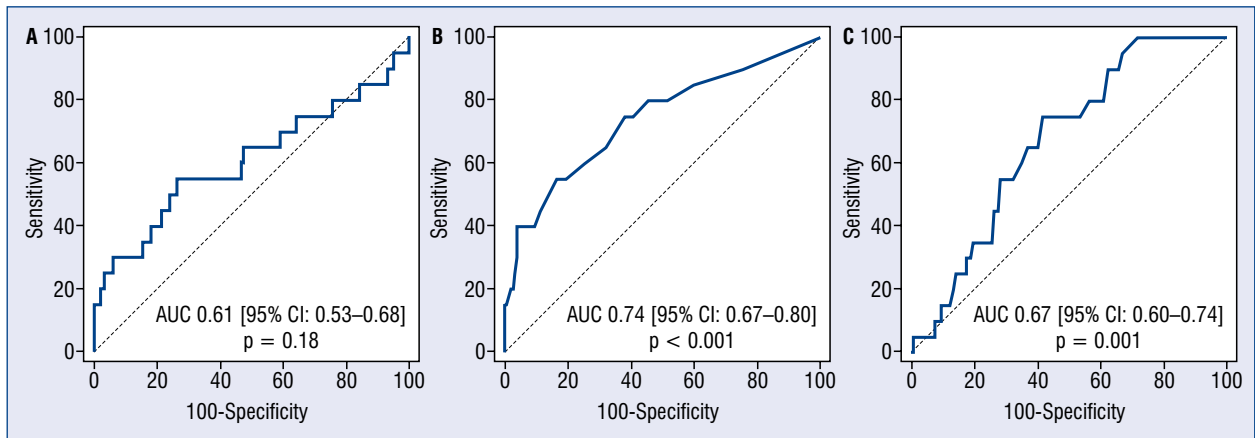


Figure 3. Receiver operation characteristic curves of post-procedural Murray law-based quantitative flow ratio (μ QFR) measurements and diameter stenosis for the prediction of vessel-oriented composite endpoint (VOCE). Receiver operator characteristic curves for the VOCE; **A.** Post-procedure diameter stenosis (AUC 0.61, 95% CI 0.53–0.68; $p = 0.18$); **B.** Post-procedural μ QFR (AUC 0.74, 95% CI 0.67–0.80; $p < 0.001$); **C.** Post-procedural μ QFR improvement (AUC 0.67, 95% CI 0.60–0.74, $p = 0.001$); AUC — area under curve; CI — confidence interval.

Table 3. Clinical outcomes stratified by the cut-off value of post-procedural Murray law-based quantitative flow ratio (μ QFR) at vessel level.

Variables	μ QFR ≤ 0.89 (n = 36)	μ QFR > 0.89 (n = 133)	P
Cardiac death	1 (2.78%)	0 (0.00%)	0.21
Target vessel MI	2 (5.56%)	0 (0.00%)	0.04
Target vessel revascularization	10 (27.78%)	9 (6.77%)	0.001
Target lesion revascularization	7 (19.44%)	8 (6.01%)	0.02
VOCE	11 (30.55%)	9 (6.77%)	< 0.001

Patients with more than one event are counted only once for the composite endpoint, although each event is listed separately. P values less than 0.05 are in bold; MI — myocardial infarction; VOCE — vessel-oriented composite endpoint

the prognostic value of Murray law-based QFR, empowered by artificial intelligence, after DCB-ISR treatment for the first time. A low μ QFR after DCB-ISR angioplasty was an independent predictor of clinical adverse events at 1-year follow-up. Post-procedural μ QFR showed an optimal predictive value for the occurrence of VOCE, and a moderate predictive value was also observed for μ QFR improvement.

Coronary interventions have classically relied on the assessment of anatomic stenosis observed in angiography, even though the stenosis severity scarcely correlates with the physiological significance as a flow-limiting lesion [24, 25] and has modest predictive value for future clinical events [26]. Decision-making based on physiology has consistently proven its superiority over purely angiographic guidance in most clinical scenarios of stable coronary heart disease, thus being endorsed

in international guidelines for clinical practice as the highest standard of care [27, 28]. The QFR is a novel tool to derive physiology parameters in the coronary arteries, based on 3D angiographic reconstruction and computerized hemodynamic simulation. This emerging method can efficiently identify functionally significant lesions, whilst overcoming the drawbacks of traditional wire-based invasive physiology [14, 15]. Previous studies have demonstrated that post-procedural QFR is significantly associated with clinical outcomes after percutaneous coronary intervention (PCI) [19, 29]. In the present study, we applied the most advanced and refined version of QFR, called Murray-law based QFR (μ QFR), which is characterized by calculating the reference vessel diameter according to fractal geometry. This adds extra accuracy to the estimation, especially for challenging bifurcation lesions, thus achieving excellent agreement with fractional flow reserve [22].

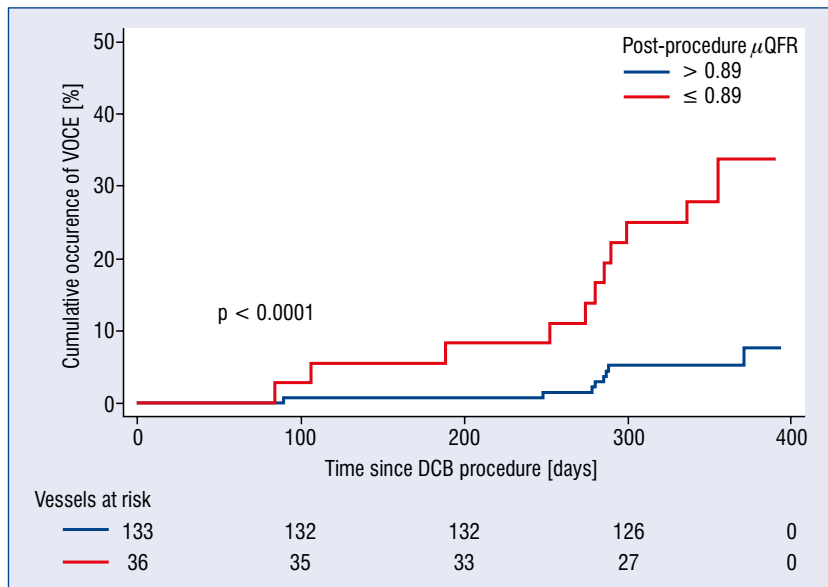


Figure 4. Kaplan-Meier curves of vessel-oriented composite endpoint (VOCE) occurrence at 1-year follow-up stratified by the best cut-off of post-procedural quantitative flow ratio (μ QFR). Blue line means vessels with post-procedure μ QFR above 0.89. Yellow line means vessels with values equal to or less than 0.89. The cut-off value of 0.89 was derived from receiver operator characteristic curve analysis for the best prediction of the VOCE; DCB — drug-coated balloon.

Table 4. Multivariable Cox regression analysis for predicting vessel-oriented composite endpoint (n = 20).

	HR (95% CI)	P
Model a1		
Post-procedural μ QFR	5.94 (2.33–15.09)	< 0.001
Diabetes mellitus	2.64 (1.03–6.78)	0.04
Difference of DCB diameter and RVD (per 0.10-mm increase)	1.34 (1.10–1.62)	0.003
Model a2		
Post-procedural μ QFR (per 0.10-mm increase)	0.34 (0.23–0.51)	< 0.001
Diabetes mellitus	1.61 (0.55–4.66)	0.16
Difference of DCB diameter and RVD (per 0.10-mm increase)	1.25 (1.03–1.50)	0.02
Model b1		
μ QFR improvement	3.75 (1.31–10.68)	0.01
Diabetes mellitus	3.15 (1.23–8.05)	0.02
Residual lesion after DCB treatment	3.12 (1.21–8.03)	0.02
Difference of DCB diameter and RVD (per 0.10-mm increase)	1.33 (1.11–1.59)	0.002
Model b2		
μ QFR improvement (per 0.10-mm increase)	1.31 (1.04–1.66)	0.02
Diabetes mellitus	3.10 (1.21–7.92)	0.02
Residual lesion after DCB treatment	3.75 (1.47–9.56)	0.01
Difference of DCB diameter and RVD (per 0.10-mm increase)	1.32 (1.11–1.57)	0.001

Independent predictors of the previous analysis were used in time-to-event analysis fitting Cox regression models with forward likelihood ratio variable selection method; p values less than 0.05 are in bold; CI — confidence interval; HR — hazard ratio; DCB — drug-coated balloon; RVD — reference vessel diameter; μ QFR — Murray law-based quantitative flow ratio

Our study proved an inverse relationship between post-procedural μ QFR and adverse clinical events after treatment of DES-ISR with DCB, an association that could not however be verified for post-procedural %DS. This finding is in line with a large corpus of evidence consistently proving the superiority of morphofunctional or computational methods over purely morphologic approaches to assess severity and prognosis [14, 16, 30]. Angiographic residual %DS has been regularly used for the assessment of procedural success in routine clinical practice [31], even though its prognostic value for future clinical events might be disputable [32]. Among morphofunctional parameters, post-procedural μ QFR showed the best prognostic value for VOCE at 1-year follow-up, superior to other parameters like μ QFR improvement. These findings clearly point out the paramount importance of functional residual lesion after treatment, in this case assessed by means of post-procedural μ QFR, and hence indirectly suggest the need to optimize the functional (rather than the angiographic) result after PCI, in line with multiple studies.

Besides functional residual stenosis, i.e., post-procedural μ QFR, and the subsequent importance of PCI optimization, an adequate DCB sizing seems also to play a relevant role for future events [33]. Obviously, an insufficient DCB balloon sizing might result in incomplete surface contact, and ultimately to inappropriate drug transfer onto the vessel wall. Nonetheless, the current study showed that the larger the oversizing of DCB diameter in regard to RVD, the higher the risk of developing VOCE at 1-year follow-up. An oversized DCB might create edge dissections of inflicting additional insult to the vessel, which might interfere with the optimal healing process, thus creating the substrate for future events. Intracoronary imaging is currently the best ancillary tool available for both accurate sizing and targeted PCI optimization, so it might be instrumental to optimize these two variables identified by our study as predictors for clinical events after treatment of DES-ISR with a DCB, namely, post-procedural μ QFR and DCB diameter mismatch. Evidence about the clinical correlates of a refined interplay between physiology and intracoronary imaging to optimize PCI results is becoming increasingly strong [34].

As in many other publications, diabetes mellitus was also an independent risk factor for adverse events in the current study, probably due to a multifactorial etiology. Diabetes has been associated with more intense plaque progression and has

been shown to elicit an exaggerated neointimal hyperplasia reaction [35, 36]. Like other clinical scenarios, the percutaneous treatment of ISR in diabetes patients is particularly challenging and deserves careful attention.

Limitations of the study

There are several limitations in the current study. First, this study is a post-hoc analysis of a previous DCB-ISR trial, which was not initially designed to investigate the prognostic value of μ QFR on ISR. Therefore, some cases did not meet the acquisition requirements for μ QFR computation. Nonetheless, this attrition of the initial sample size occurred at random and was therefore unlikely to result in selection bias. All cases were analyzed off-line, which inevitably affects the precise analysis. Second, the cut-off value of post-procedural μ QFR to predict vessel-oriented composite events was not exclusive, varied widely due to multiple factors, including the observed population, incidence of clinical events, lesion and procedural characteristics, etc., and should be validated in a future large randomized controlled trial. Lastly, intravascular imaging was not mandatory in the previous trial; conversely, intravascular morphology information would be beneficial to understand the underlying mechanics of low μ QFR values and adverse events.

Conclusions

Post-procedural μ QFR after treatment of ISR with DCB was inversely associated with the occurrence of subsequent adverse clinical events and may be considered as a promising predictor.

Acknowledgments

The authors would like to thank the dedicated efforts from the clinical research collaborators who participated in the previous DCB-ISR trial.

Conflict of interest: Shengxian Tu received a research grant from Pulse Medical Imaging Technology. All other authors have reported that they have no relationships relevant to the contents of this paper to disclose.

References

1. Stettler C, Wandel S, Allemann S, et al. Outcomes associated with drug-eluting and bare-metal stents: a collaborative network meta-analysis. *Lancet*. 2007; 370(9591): 937–948, doi: [10.1016/S0140-6736\(07\)61444-5](https://doi.org/10.1016/S0140-6736(07)61444-5), indexed in Pubmed: [17869634](https://pubmed.ncbi.nlm.nih.gov/17869634/).

2. Stone G, Moses J, Ellis S, et al. Safety and efficacy of sirolimus- and paclitaxel-eluting coronary stents. *N Engl J Med.* 2007; 356(10): 998–1008, doi: [10.1056/nejmoa067193](https://doi.org/10.1056/nejmoa067193).
3. Dangas GD, Claessen BE, Caixeta A, et al. In-stent restenosis in the drug-eluting stent era. *J Am Coll Cardiol.* 2010; 56(23): 1897–1907, doi: [10.1016/j.jacc.2010.07.028](https://doi.org/10.1016/j.jacc.2010.07.028), indexed in Pubmed: [21109112](https://pubmed.ncbi.nlm.nih.gov/21109112/).
4. Alfonso F, Byrne RA, Rivero F, et al. Current treatment of in-stent restenosis. *J Am Coll Cardiol.* 2014; 63(24): 2659–2673, doi: [10.1016/j.jacc.2014.02.545](https://doi.org/10.1016/j.jacc.2014.02.545), indexed in Pubmed: [24632282](https://pubmed.ncbi.nlm.nih.gov/24632282/).
5. Scheller B, Clever YP, Kelsch B, et al. Treatment of coronary in-stent restenosis with a paclitaxel-coated balloon catheter. *N Engl J Med.* 2006; 355(20): 2113–2124, doi: [10.1056/NEJMoa061254](https://doi.org/10.1056/NEJMoa061254), indexed in Pubmed: [17101615](https://pubmed.ncbi.nlm.nih.gov/17101615/).
6. Unverdorben M, Vallbracht C, Cremers B, et al. Paclitaxel-coated balloon catheter versus paclitaxel-coated stent for the treatment of coronary in-stent restenosis. *Circulation.* 2009; 119(23): 2986–2994, doi: [10.1161/CIRCULATIONAHA.108.839282](https://doi.org/10.1161/CIRCULATIONAHA.108.839282), indexed in Pubmed: [19487593](https://pubmed.ncbi.nlm.nih.gov/19487593/).
7. Adriaenssens T, Dens Jo, Ughi G, et al. Optical coherence tomography study of healing characteristics of paclitaxel-eluting balloons vs. everolimus-eluting stents for in-stent restenosis: the SEDUCE (Safety and Efficacy of a Drug eluting balloon in Coronary artery rEstenosis) randomised clinical trial. *EuroIntervention.* 2014; 10(4): 439–448, doi: [10.4244/EIJV10I4A77](https://doi.org/10.4244/EIJV10I4A77), indexed in Pubmed: [25138182](https://pubmed.ncbi.nlm.nih.gov/25138182/).
8. Pleva L, Kukla P, Kusnierova P, et al. Comparison of the efficacy of paclitaxel-eluting balloon catheters and everolimus-eluting stents in the treatment of coronary in-stent restenosis: the treatment of in-stent restenosis study. *Circ Cardiovasc Interv.* 2016; 9(4): e003316, doi: [10.1161/CIRCINTERVENTIONS.115.003316](https://doi.org/10.1161/CIRCINTERVENTIONS.115.003316), indexed in Pubmed: [27069104](https://pubmed.ncbi.nlm.nih.gov/27069104/).
9. Giacoppo D, Matsuda Y, Fovino LN, et al. Short dual antiplatelet therapy followed by P2Y12 inhibitor monotherapy vs. prolonged dual antiplatelet therapy after percutaneous coronary intervention with second-generation drug-eluting stents: a systematic review and meta-analysis of randomized clinical trials. *Eur Heart J.* 2021; 42(4): 308–319, doi: [10.1093/eurheartj/ehaa739](https://doi.org/10.1093/eurheartj/ehaa739), indexed in Pubmed: [33284979](https://pubmed.ncbi.nlm.nih.gov/33284979/).
10. Chen Y, Gao L, Qin Q, et al. Comparison of 2 different drug-coated balloons in in-stent restenosis: the RESTORE ISR China randomized trial. *JACC Cardiovasc Interv.* 2018; 11(23): 2368–2377, doi: [10.1016/j.jcin.2018.09.010](https://doi.org/10.1016/j.jcin.2018.09.010), indexed in Pubmed: [30522665](https://pubmed.ncbi.nlm.nih.gov/30522665/).
11. Zhu J, Liu L, Zhu Z, et al. A randomized comparison of a novel iopromide-based paclitaxel-coated balloon Shenqi versus SeQuent Please for the treatment of in-stent restenosis. *Coron Artery Dis.* 2021; 32(6): 526–533, doi: [10.1097/MCA.0000000000000994](https://doi.org/10.1097/MCA.0000000000000994), indexed in Pubmed: [33229940](https://pubmed.ncbi.nlm.nih.gov/33229940/).
12. Xu Bo, Gao R, Wang J, et al. A prospective, multicenter, randomized trial of paclitaxel-coated balloon versus paclitaxel-eluting stent for the treatment of drug-eluting stent in-stent restenosis: results from the PEPCAD China ISR trial. *JACC Cardiovasc Interv.* 2014; 7(2): 204–211, doi: [10.1016/j.jcin.2013.08.011](https://doi.org/10.1016/j.jcin.2013.08.011), indexed in Pubmed: [24556098](https://pubmed.ncbi.nlm.nih.gov/24556098/).
13. Giacoppo D, Alfonso F, Xu Bo, et al. Drug-Coated balloon angioplasty versus drug-eluting stent implantation in patients with coronary stent restenosis. *J Am Coll Cardiol.* 2020; 75(21): 2664–2678, doi: [10.1016/j.jacc.2020.04.006](https://doi.org/10.1016/j.jacc.2020.04.006), indexed in Pubmed: [32466881](https://pubmed.ncbi.nlm.nih.gov/32466881/).
14. Tu S, Barbato E, Köszegi Z, et al. Fractional flow reserve calculation from 3-dimensional quantitative coronary angiography and TIMI frame count: a fast computer model to quantify the functional significance of moderately obstructed coronary arteries. *JACC Cardiovasc Interv.* 2014; 7(7): 768–777, doi: [10.1016/j.jcin.2014.03.004](https://doi.org/10.1016/j.jcin.2014.03.004), indexed in Pubmed: [25060020](https://pubmed.ncbi.nlm.nih.gov/25060020/).
15. Xu Bo, Tu S, Qiao S, et al. Diagnostic accuracy of angiography-based quantitative flow ratio measurements for online assessment of coronary stenosis. *J Am Coll Cardiol.* 2017; 70(25): 3077–3087, doi: [10.1016/j.jacc.2017.10.035](https://doi.org/10.1016/j.jacc.2017.10.035), indexed in Pubmed: [29101020](https://pubmed.ncbi.nlm.nih.gov/29101020/).
16. Tu S, Westra J, Yang J, et al. Diagnostic accuracy of fast computational approaches to derive fractional flow reserve from diagnostic coronary angiography: the international multicenter FAVOR pilot study. *JACC Cardiovasc Interv.* 2016; 9(19): 2024–2035, doi: [10.1016/j.jcin.2016.07.013](https://doi.org/10.1016/j.jcin.2016.07.013), indexed in Pubmed: [27712739](https://pubmed.ncbi.nlm.nih.gov/27712739/).
17. Asano T, Katagiri Y, Collet C, et al. Functional comparison between the BuMA Supreme biodegradable polymer sirolimus-eluting stent and a durable polymer zotarolimus-eluting coronary stent using quantitative flow ratio: PIONEER QFR substudy. *EuroIntervention.* 2018; 14(5): e570–e579, doi: [10.4244/EIJ-D-17-00461](https://doi.org/10.4244/EIJ-D-17-00461), indexed in Pubmed: [28994655](https://pubmed.ncbi.nlm.nih.gov/28994655/).
18. Lontou C, Mejía-Rentería H, Lauri F, et al. Quantitative flow ratio for functional evaluation of in-stent restenosis. *EuroIntervention.* 2021; 17(5): e396–e398, doi: [10.4244/eij-d-18-00955](https://doi.org/10.4244/eij-d-18-00955).
19. Biscaglia S, Tebaldi M, Brugaletta S, et al. Prognostic value of QFR measured immediately after successful stent implantation: the international multicenter prospective HAWKEYE study. *JACC Cardiovasc Interv.* 2019; 12(20): 2079–2088, doi: [10.1016/j.jcin.2019.06.003](https://doi.org/10.1016/j.jcin.2019.06.003), indexed in Pubmed: [31563688](https://pubmed.ncbi.nlm.nih.gov/31563688/).
20. Cai X, Tian F, Jing J, et al. Prognostic value of quantitative flow ratio measured immediately after drug-coated balloon angioplasty for in-stent restenosis. *Catheter Cardiovasc Interv.* 2021; 97 Suppl 2: 1048–1054, doi: [10.1002/ccd.29640](https://doi.org/10.1002/ccd.29640), indexed in Pubmed: [33742738](https://pubmed.ncbi.nlm.nih.gov/33742738/).
21. Tang J, Hou H, Chu J, et al. Clinical implication of quantitative flow ratio to predict clinical events after drug-coated balloon angioplasty in patients with in-stent restenosis. *Clin Cardiol.* 2021; 44(7): 978–986, doi: [10.1002/clc.23630](https://doi.org/10.1002/clc.23630), indexed in Pubmed: [34009672](https://pubmed.ncbi.nlm.nih.gov/34009672/).
22. Tu S, Ding D, Chang Y, et al. Diagnostic accuracy of quantitative flow ratio for assessment of coronary stenosis significance from a single angiographic view: A novel method based on bifurcation fractal law. *Catheter Cardiovasc Interv.* 2021; 97 Suppl 2: 1040–1047, doi: [10.1002/ccd.29592](https://doi.org/10.1002/ccd.29592), indexed in Pubmed: [33660921](https://pubmed.ncbi.nlm.nih.gov/33660921/).
23. Mehran R, Dangas G, Abizaid AS, et al. Angiographic patterns of in-stent restenosis: classification and implications for long-term outcome. *Circulation.* 1999; 100(18): 1872–1878, doi: [10.1161/01.cir.100.18.1872](https://doi.org/10.1161/01.cir.100.18.1872), indexed in Pubmed: [10545431](https://pubmed.ncbi.nlm.nih.gov/10545431/).
24. Meijboom WB, Van Mieghem CAG, van Pelt N, et al. Comprehensive assessment of coronary artery stenoses: computed tomography coronary angiography versus conventional coronary angiography and correlation with fractional flow reserve in patients with stable angina. *J Am Coll Cardiol.* 2008; 52(8): 636–643, doi: [10.1016/j.jacc.2008.05.024](https://doi.org/10.1016/j.jacc.2008.05.024), indexed in Pubmed: [18702967](https://pubmed.ncbi.nlm.nih.gov/18702967/).
25. Toth G, Hamilos M, Pyxaras S, et al. Evolving concepts of angiogram: fractional flow reserve discordances in 4000 coronary stenoses. *Eur Heart J.* 2014; 35(40): 2831–2838, doi: [10.1093/eurheartj/ehu094](https://doi.org/10.1093/eurheartj/ehu094), indexed in Pubmed: [24644308](https://pubmed.ncbi.nlm.nih.gov/24644308/).
26. Nunen Lv, Zimmermann F, Tonino P, et al. Fractional flow reserve versus angiography for guidance of PCI in patients with multivessel coronary artery disease (FAME): 5-year follow-up of a randomised controlled trial. *Lancet.* 2015; 386(10006): 1853–1860, doi: [10.1016/s0140-6736\(15\)00057-4](https://doi.org/10.1016/s0140-6736(15)00057-4).

27. Levine GN, Bates ER, Blankenship JC, et al. 2011 ACCF/AHA/SCAI Guideline for Percutaneous Coronary Intervention: executive summary: a report of the American College of Cardiology Foundation/American Heart Association Task Force on Practice Guidelines and the Society for Cardiovascular Angiography and Interventions. *Circulation*. 2011; 124(23): 2574–2609, doi: [10.1161/CIR.0b013e31823a5596](https://doi.org/10.1161/CIR.0b013e31823a5596), indexed in Pubmed: [22064598](https://pubmed.ncbi.nlm.nih.gov/22064598/).
28. NEUMANN FJ, SOUSA-UVA M, AHLSSON A, et al. 2018 ESC/EACTS Guidelines on myocardial revascularization. *Eur Heart J*. 2019; 40(2): 87–165, doi: [10.1093/eurheartj/ehy394](https://doi.org/10.1093/eurheartj/ehy394), indexed in Pubmed: [30165437](https://pubmed.ncbi.nlm.nih.gov/30165437/).
29. Ding D, Huang J, Westra J, et al. Immediate post-procedural functional assessment of percutaneous coronary intervention: current evidence and future directions. *Eur Heart J*. 2021; 42(27): 2695–2707, doi: [10.1093/eurheartj/ehab186](https://doi.org/10.1093/eurheartj/ehab186), indexed in Pubmed: [33822922](https://pubmed.ncbi.nlm.nih.gov/33822922/).
30. Gutiérrez-Chico JL, Chen Y, Yu W, et al. Diagnostic accuracy and reproducibility of optical flow ratio for functional evaluation of coronary stenosis in a prospective series. *Cardiol J*. 2020; 27(4): 350–361, doi: [10.5603/CJ.a2020.0071](https://doi.org/10.5603/CJ.a2020.0071), indexed in Pubmed: [32436590](https://pubmed.ncbi.nlm.nih.gov/32436590/).
31. Bech GJ, Pijls NH, De Bruyne B, et al. Usefulness of fractional flow reserve to predict clinical outcome after balloon angioplasty. *Circulation*. 1999; 99(7): 883–888, doi: [10.1161/01.cir.99.7.883](https://doi.org/10.1161/01.cir.99.7.883), indexed in Pubmed: [10027810](https://pubmed.ncbi.nlm.nih.gov/10027810/).
32. Lee JM, Hwang D, Choi KiH, et al. Prognostic impact of residual anatomic disease burden after functionally complete revascularization. *Circ Cardiovasc Interv*. 2020; 13(9): e009232, doi: [10.1161/CIRCINTERVENTIONS.120.009232](https://doi.org/10.1161/CIRCINTERVENTIONS.120.009232), indexed in Pubmed: [32895005](https://pubmed.ncbi.nlm.nih.gov/32895005/).
33. Yerasi C, Case BC, Forrestal BJ, et al. Drug-coated balloon for de novo coronary artery disease: JACC state-of-the-art review. *J Am Coll Cardiol*. 2020; 75(9): 1061–1073, doi: [10.1016/j.jacc.2019.12.046](https://doi.org/10.1016/j.jacc.2019.12.046), indexed in Pubmed: [32138967](https://pubmed.ncbi.nlm.nih.gov/32138967/).
34. Kedhi E, Berta B, Roleder T, et al. Thin-cap fibroatheroma predicts clinical events in diabetic patients with normal fractional flow reserve: the COMBINE OCT-FFR trial. *Eur Heart J*. 2021 [Epub ahead of print], doi: [10.1093/eurheartj/ehab433](https://doi.org/10.1093/eurheartj/ehab433), indexed in Pubmed: [34345911](https://pubmed.ncbi.nlm.nih.gov/34345911/).
35. Yang ZK, Shen Y, Dai Y, et al. Impact of coronary collateralization on long-term clinical outcomes in type 2 diabetic patients after successful recanalization of chronic total occlusion. *Cardiovasc Diabetol*. 2020; 19(1): 59, doi: [10.1186/s12933-020-01033-4](https://doi.org/10.1186/s12933-020-01033-4), indexed in Pubmed: [32393276](https://pubmed.ncbi.nlm.nih.gov/32393276/).
36. Shi R, Shi Ke, Yang ZG, et al. Serial coronary computed tomography angiography-verified coronary plaque progression: comparison of stented patients with or without diabetes. *Cardiovasc Diabetol*. 2019; 18(1): 123, doi: [10.1186/s12933-019-0924-z](https://doi.org/10.1186/s12933-019-0924-z), indexed in Pubmed: [31551077](https://pubmed.ncbi.nlm.nih.gov/31551077/).